A COMPARISON OF INFLATABLE AND SEMI-RIGID DEPLOYABLE AERODYNAMIC DECELERATORS FOR FUTURE AEROCAPTURE AND ENTRY MISSIONS

Reuben R. Rohrschneider, Jim Masciarelli, and Kevin L. Miller

Ball Aerospace & Technologies Corp., 1600 Commerce St, Boulder CO 80301, [rrohrsch,jmasciar,klmiller]@ball.com

Abstract

With the successful flight of Inflatable Reentry Vehicle Experiment-II, the concept of using fabric-based aerodynamic decelerators has been demonstrated. This flight was a ballistic entry from a sub-orbital velocity. Now, with the imminent launch of the Mars Science Laboratory and its guided lifting aeroshell, the bar has been raised for all future aerodynamic decelerator systems. Once this technology has been successfully demonstrated, future science missions will demand precision landing from any entry system, including future deployable aerodynamic decelerators. The Entry, Descent and Landing Systems Analysis (EDL-SA) study compared hypersonic inflatable aerodynamic decelerators to a rigid design, and found the architectures using rigid entry systems slightly better than the deployable system studied. This paper compares different deployable entry systems, including both inflatable and semi-rigid designs, to examine if the stacked torus configuration used in the EDL-SA study was the best choice. This study found that a semi-rigid configuration with rigid radial spars offers significant advantages over the stacked torus configuration when using the same top-level evaluation criteria and weights as the EDL-SA study.

Nomenclature

AHP	= Analytic hierarchy process
EDL-SA	= Entry, Descent, and Landing Systems Analysis
HIAD	= Hypersonic inflatable aerodynamic decelerator
HMMES	= High-mass Mars entry systems
IRVE	= Inflatable Reentry Vehicle Experiment
LCC	= Life cycle cost
MOLA	= Mars Orbital Laser Altimeter
MSL	= Mars Science Laboratory
mt	= Metric ton
NASA	= National Aeronautics and Space Administration
PESST	= Planetary Entry Systems Synthesis Tool
R&D^3	= Research and development degree of difficulty
RRS	= Rigid radial spars
ST	= Stacked torus
TC	= Tension cone
TPS	= Thermal protection system
TRL	= Technology readiness level
TT	= Trailing torus

Introduction

The current state-of-the-art for Mars entry systems uses a rigid aeroshell for hypersonic deceleration, a disk-gap-band parachute deployed near Mach 2.0, and either airbags or chemical propulsion for terminal descent. This entry architecture is representative of all the successful United States Mars missions flown to date, with a maximum entry mass less than 1000 kg (590 kg payload) and landed altitude of -1.4 km referenced to the Mars Orbital Laser Altimeter (MOLA). With the successful flight of the Mars Science Laboratory (MSL) the envelope will be extended to nearly 3000 kg entry mass (800 kg payload) and +2.0 km MOLA landing altitude. Braun and Manning[i] show that this is very near the limit of the current landing architecture, and that new technology will be needed for larger missions. One option for this new technology is the deployable aerodynamic decelerator, which prior studies have shown offers substantial mass advantages to rigid systems at Mars, and other destinations with an atmosphere, for both entry and aerocapture[ii,iii]. Furthermore, deployable systems promise a much broader range of landing altitudes and entry masses that support human exploration.

There are multiple deployable aerodynamic decelerator concepts that can be divided into two primary classes: inflatables, and semi-rigid deployables. The two main classes of deployable aerodynamic decelerator have been compared for both aerocapture and entry at Mars using ballistic trajectories, and their entry system mass fractions were shown to be within 4%[iv]. With such similar mass performance, other metrics such as precision landing capability, resistance to micrometeoroids, and operational flexibility should be considered when planning future technology investments in aerodynamic decelerators. The Entry, Descent and Landing Systems Analysis (EDL-SA) study performed this analysis for different entry architectures at Mars, including rigid, propulsive, and deployable systems, and provided a set of evaluation categories and weights based on interviews with NASA program managers. The study concluded that their choice of rigid entry vehicle (the ellipsled) was slightly preferred over their choice of deployable entry system (the stacked torus inflatable). The past experience of the authors and the results of the high mass Mars entry system (HMMES) study indicate that the choice of the stacked torus inflatable may not be the best option.

This paper draws from the results of the HMMES study and the EDL-SA study to compare four different deployable entry systems using the evaluation criteria outlined in the EDL-SA study. This paper is organized into two main sections. The first section provides an overview of the methods and results of the HMMES study, and is followed by an evaluation of the deployable configurations and the rationale behind the rankings and the conclusions.

Summary of the HMMES Deployable Entry System Study

Of the many different deployable configurations in the literature this study limits itself to configurations applicable to hypersonic entry. Initial configurations were taken from the open literature and 5 of these configurations were selected for inclusion in a systems study. The evaluation criteria and metrics used for configuration selection are presented in Table 1. The result of this down-select are the configurations shown in Figure 1. The selection includes five deployable configurations and one rigid configuration for comparison to other studies.

Table 1. Evaluation criteria and weight factors used to select configurations for the systems study.

Evaluation Criteria	Weighting Factor (Normalized)
Potential for developing L/D	**0.18**
Scalability to large sizes	**0.13**
Entry system mass fraction	**0.24**
Usable payload volume	**0.13**
Ease of design & construction	**0.13**
Reliability & durability	**0.18**

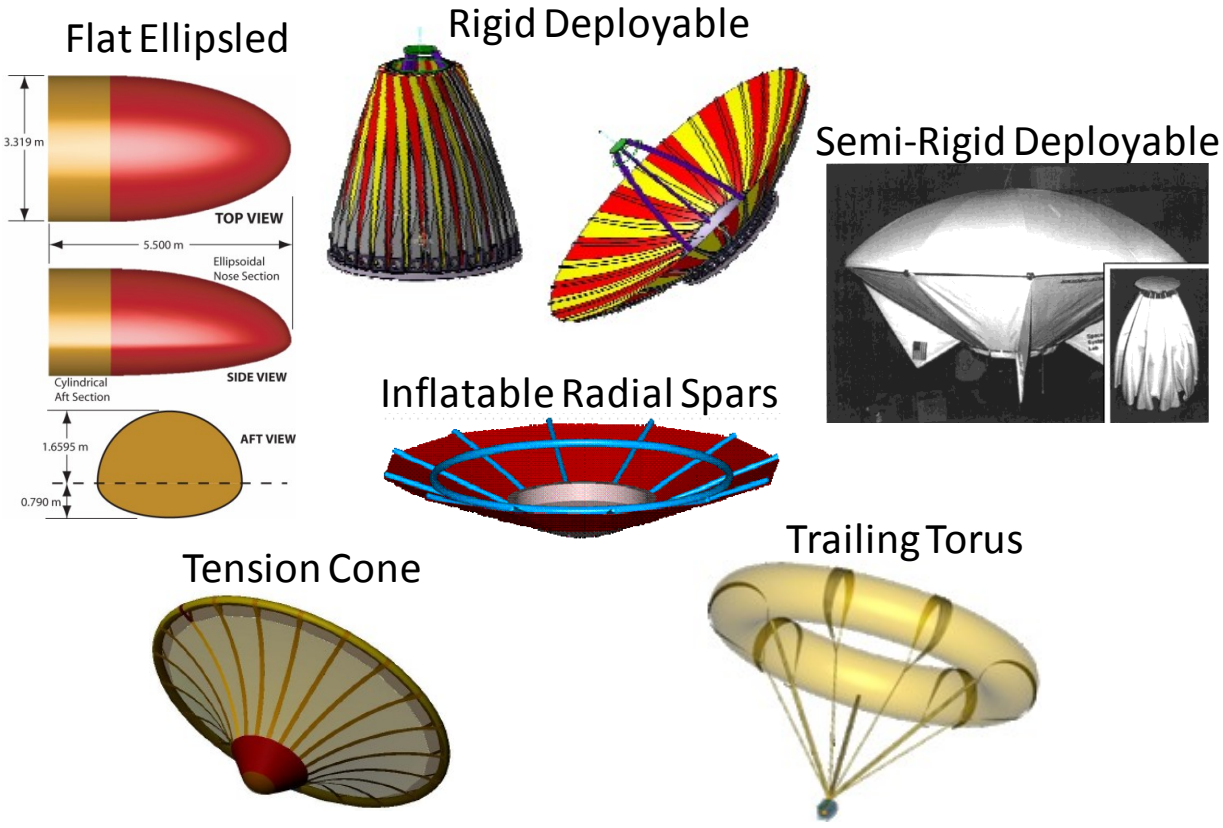

Figure 1. Configurations selected for the systems study. [ii,vi,vii,ix,xi,xii]

Analysis models for each of the six configurations were developed in more detail, including parametric outer mold line geometry, parametric mass models, and thermal models. The configurations were added to the Planetary Entry Systems Synthesis Tool[v] (PESST) to automate the analysis process and allow optimization of each configuration at 4, 10, 40, 60, and 100 metric ton entry masses. All configurations used a propulsive terminal descent system with gravity turn guidance to a soft landing at 0 km MOLA. The only configuration that produces lift is the flat ellipsled. The remaining configurations are symmetric about their centers of mass and have sufficiently low ballistic coefficients to produce feasible entry

systems using ballistic entry. All configurations are assumed to carry a cylindrical payload canister with structural integrity of its own, which contains the payload and all non-entry systems. Each configuration is described in more detail below.

Flat Ellipsled

The flat ellipsled configuration was developed for Neptune aerocapture, and produced a lighter thermal protection system than a cylindrical ellipsled[vi] due to the larger effective nose radius. The geometry of the flat ellipsled consists of a cylindrical top section and an elliptical lower section, joined where the slope of each section is vertical. For the systems study the flat ellipsled geometry is photographically scaled based on the 5.5m design.

The flat ellipsled structure consists of a rigid shell covered with insulation and an ablative thermal protection system (TPS). The ablative TPS thickness and insulation are resized using a transient heating calculation for each entry condition to avoid overestimating the TPS mass.

The entry trajectory has a set initial bank angle, and at a time specified by the optimizer this rotates towards zero (full lift up) linearly with dynamic pressure. Two other methods were tested, but produced heavier vehicles.

For the flat ellipsled configuration the optimizer controls the scale factor of the vehicle, the entry bank angle, and the time to start rotating the bank angle to zero. The angle of attack was fixed specifically to keep the vehicle in a regime with a larger effective nose radius to reduce heating.

Rigid Deployable

The rigid deployable configuration consists of a central heatshield that is sized as if it was a rigid capsule with ablative TPS, and panels that fold down around the perimeter of the central heatshield to form a 60 degree half-angle cone[vii]. The panels are cantilevered from a deployment spring and latching mechanism and are constructed of C/SiC facesheets with carbon foam core.

The data available for C/SiC[viii] indicates that the strength increases with increasing temperature up to 1500 deg C. No data was presented beyond this temperature, so 1500 deg C was assumed to be the material's operating temperature limit. Assuming a surface emissivity of 0.85 and one-sided radiation, a 63 W/cm^2 heat rate limit was found to produce a radiative equilibrium temperature of 1500 deg C. The 63 W/cm^2 heat rate is used as a constraint during optimization.

During optimization the only geometric control variable is a scale factor that determines the overall size of the vehicle.

Rigid Radial Spars

The rigid radial spars configuration is representative of the semi-rigid class of deployables, and consists of a central heatshield, which is sized like a rigid capsule, and aluminum wrapped carbon fiber composite radial spars that support Nextel 312AF-10 fabric between them. The configuration looks much like an umbrella. The rigid radial spar (RRS) configuration was built and tested prior to a failed launch attempt by the Massachusetts Institute of Technology[ix].

Detailed thermal analysis of the design indicates a maximum allowable heat rate of 16 W/cm^2, which is used as a constraint during optimization[x]. The model used for the systems study includes an insulation

model based on Fibermax mat insulation instead of the extra layers of Nextel fabric specified in the literature.

The deployment mechanism is altered slightly from the documented lead screw to use a winch and cable mechanism that pulls a conical latching mechanism into a receptacle on the front of the payload canister. This would shift the heatshield closer to the payload and require mounting of the struts to the side, rather than the front, of the payload canister. Shifting the payload closer to the heatshield also serves to improve vehicle stability.

The Parashield configuration has two geometric design variables that the optimizer controls: scale factor, and nose radius.

Radial Inflated Spars

The radial inflated spar configuration consists of radial inflatable beams with membrane material stretched between them, and an inflatable torus supporting the radial beams near 2/3 of the maximum radius[xi]. The center of the vehicle is a rigid spherical heatshield with structure, and the radial spars form a 60 degree half-angle cone.

The membrane stretched between radial spars is made of Upilex, and the inflatable portions of the design use a Upilex bladder overwrapped with braided Technora fiber and Vectran reinforcing straps. All of these material properties are reduced to 20% of room temperature strength to account for operating at 500 deg C. The beam diameter, torus diameter, and number of radial beams are iterated to determine the values that minimize overall system mass.

Given the 500 degree C operating temperature limit on the membrane, the heat rate limit was found to be 4.5 W/cm^2 on the nose. The limit was determined using the radiative equilibrium temperature and assuming an emissivity of 0.85 and two-sided radiation. The resulting heat rate was then divided by the cosine of 60 deg to account for the value being calculated at the stagnation point in the trajectory code, which effectively limits the heat rate on the membrane to 3.0 W/cm^2.

The radial inflated spar configuration only allows the optimizer to control a scale factor that changes the overall vehicle diameter. Number of radial beams and diameter of inflatable components is optimized within the structural analysis.

Tension Cone

The tension cone (TC) configuration consists of an inflated torus with radial straps connecting it to a rigid aeroshell[xii]. Fabric gores are stitched between the radial straps to form a continuous surface between the spacecraft and torus. The radial straps carry the axial load, and the gores are only intended to carry the circumferential load induced by aerodynamic drag.

The central body is modeled as a spherical heatshield with tangency to the radial straps and includes structure and insulation mass. The radial straps are Kevlar webbing and the gores are Upilex. The torus uses an Upilex bladder overwrapped with Technora fiber and reinforcing straps. Radial straps are attached to the torus at every 4 torus minor diameters. Fibermax mat insulation is placed over the radial straps and the torus leading edge to limit the material temperature to 500 deg C while allowing a higher heating rate at the surface. Detailed thermal analysis of the tension cone configuration indicated an allowable heat rate

limit of 16 W/cm^2 on the vehicle nose[xiii] when the front of the torus is insulated and the webbing near the spacecraft is insulated.

The tension cone configuration allows the optimizer to change both a scale factor that controls overall diameter and the ratio of overall diameter divided by torus minor diameter. The torus minor diameter was not optimized in the structural analysis because the minor diameter affects overall aerodynamic properties and is controlled by the global optimizer.

Trailing Torus

The trailing torus (TT) configuration consists of a torus attached to the spacecraft with multiple tension tethers and three inflatable columns[ii]. The columns are required to position the torus while inflated in space and prevent the tension tethers from tangling.

The torus is constructed of an Upilex bladder overwrapped with Vectran fiber and Technora reinforcing straps. Eight Vectran tension tethers are used to attach the spacecraft to the torus. The torus major diameter to minor diameter ratio is fixed at 5:1, and the angle of the tension tethers is 45 deg to allow the hole in the torus to swallow the spacecraft wake[xiv]. Due to the small diameter of the tension tethers, a layer of aluminum foil and Nextel fabric insulation is required to reduce the tether temperature to acceptable levels. Detailed thermal analysis of the torus revealed that the heat rate on the leading edge of the torus must be kept below 3.0 W/cm^2 to maintain the material temperature below 500 deg C[ii]. The torus is not insulated.

The trailing torus configuration only allows the optimizer to vary a scale factor controlling overall diameter. The ratio of torus minor diameter to major diameter was fixed since the simple aerodynamics model used cannot resolve the problems associated with varying the torus ratio and location of the spacecraft relative to the torus.

Analysis Methodology

In order to compare the configurations, a baseline set of analysis conditions were selected. The entry velocity used is 7,500 m/s and represents one of the higher entry velocities used at Mars, making it a challenging case for the entry systems studied. The atmospheric interface altitude was 140 km for deployable configurations since sensible drag was observed at lower altitudes. The atmosphere density profile is taken from the Mars Pathfinder trajectory reconstruction[xv]. This dataset is publicly available and known to the entry community, facilitating comparison and reproduction of the work.

The optimizer used is the Simplex Method available in Matlab, and requires that constraints be added as exterior penalty functions. Gradient based optimizers were also explored, but they tended to step too far out of the feasible solution space, causing PESST to hang or report invalid results, hence producing bad results or optimizer errors. The Simplex method, while not fast, consistently produced good results without encountering errors. The optimization was setup to use the all-at-once method[xvi].

The objective function for all cases is the entry system mass fraction. The entry system mass includes the deployable, heatshield and insulation, descent engines and propellant masses. The entry system mass fraction divides the entry system mass by the total entry mass, making lower values more favorable.

For all optimization cases the scale factor, entry flight path angle, maximum thrust, and altitude to start the gravity turn are optimization variables. There are additional configuration specific design variables that were mentioned in the configuration descriptions above.

Analysis Results

A summary of the direct entry results for each configuration is shown in Figure 2. The configurations fall into two groupings, with the tension cone, trailing torus, and radial rigid spar configurations having significantly lower entry system mass fractions than the flat ellipsled, radial inflated spars, and rigid deployable configurations. The tension cone has the lowest entry system mass fraction, with the difference between the entry system mass fractions of the best three configurations ranging up to 4% over the entry mass range studied.

The flat ellipsled results fall in the range of a previous study of Apollo-like shapes[xvii] that calculated an entry system mass fraction between 70% and 90%. The 4 mt point on the ellipsled curve does not follow the trend because no feasible solution was found that did not violate the packing density constraint. The packing density constraint was removed for just the 4 mt analysis, and the best result is shown that meets the other constraints. The resulting packing density is 567 kg/m^3 at that point, which is unrealistically high, likely infeasible, and results in a very heavy heatshield.

The rigid deployable offers a better solution than the flat ellipsled at low entry masses, but quickly becomes worse and is infeasible for masses above 60 mt. The addition of a locking mechanism at the perimeter of the deployable could allow the structure to carry hoop loads and would likely reduce vehicle mass, though this was not included in this study. The radial inflated spar configuration does not scale well and is infeasible for entry masses over approximately 30 mt.

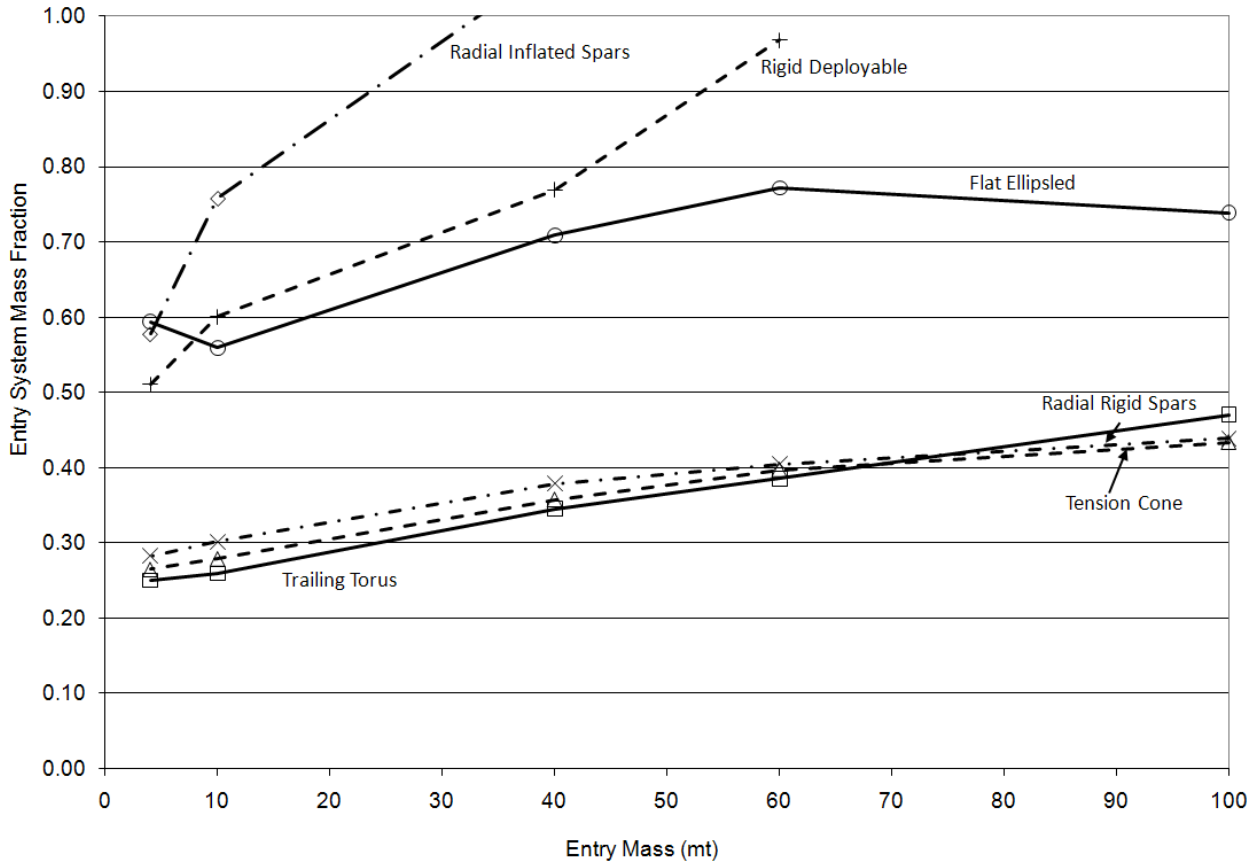

Figure 2. Summary of direct entry results for each configuration analyzed.

Deployable Design Comparison

Using the analysis results of the HMMES study and the categories and weights provided in the EDL-SA year 1 study report[xviii], the deployable entry systems are ranked using the Analytic Hierarchy Process (AHP). The goal is to compare the deployable entry systems studied here to the stacked torus (ST) hypersonic inflatable aerodynamic decelerator (HIAD) used in the EDL-SA study. The comparison will be made at the 100mt entry mass to be as close as possible to the mass regime used in the EDL-SA study, and the rigid vehicle will not be included since the EDL-SA study already provides an analysis of this configuration relative to the stacked torus HIAD. The radial inflated spar and rigid deployable configurations are also excluded since they are infeasible at the 100 mt entry mass.

The top-level evaluation criteria from the EDL-SA study are shown in Figure 3 with their sub-criteria listed below them along with their effective weights. The lowest branches of the hierarchy are where direct comparisons between each configuration are made, and the effective weight at that level is found by multiplying by the weights of all categories along that branch. Weights of sub-categories are set equal as these were not provided in the EDL-SA year 1 study report.

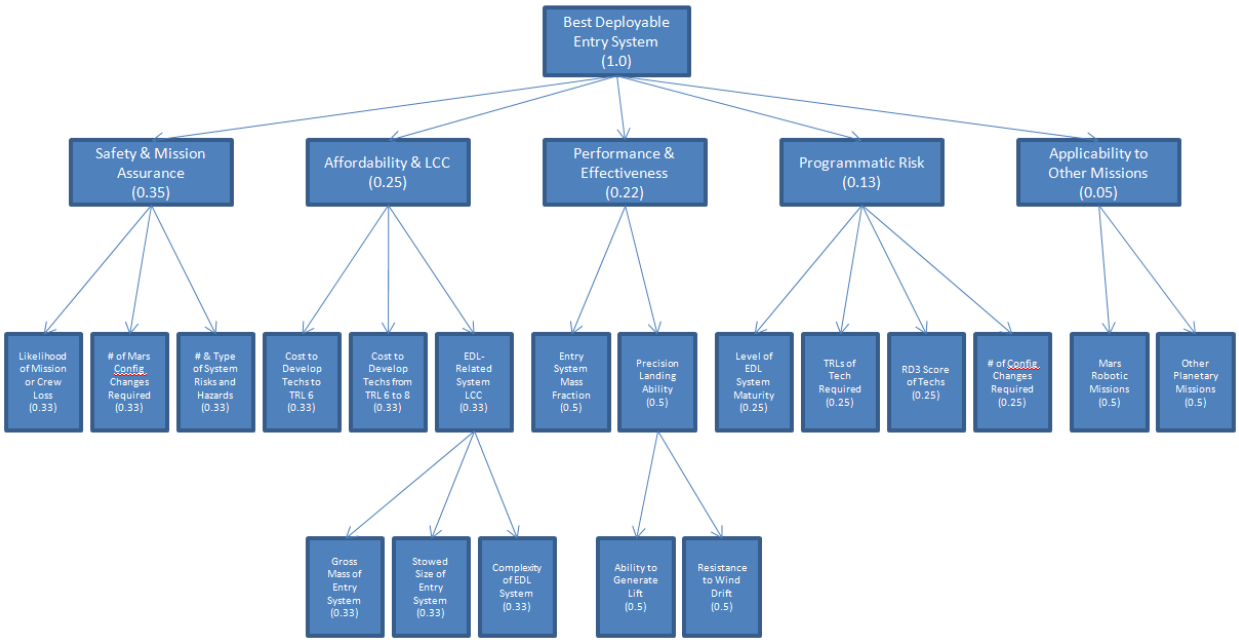

Figure 3. Hierarchy of categories used to compare the deployable entry systems and their weights within their sub-categories.

Comparison of the sub-categories in this list to the EDL-SA study will reveal some changes. This is because the EDL-SA study evaluated architectures, and categories that were specific to architecture evaluation were removed entirely, or replaced with equivalent EDL system categories. The criteria used and the rankings of each configuration will be discussed below.

The scale used for the AHP pair wise comparisons starts at a value of 1 for no discernable difference and ends at 5 for a significant difference. Only values of 1, 3, and 5 are used for qualitative comparisons.

Safety & Mission Assurance

The safety and mission assurance category contains topics related to loss of mission or crew. The chosen subtopics are abort options and redundancy, number of Mars configuration changes required, and number and type of system risks and mission hazards. A summary of the evaluations in this category is provided in Table 2 and rationales for the rankings are provided below.

Table 2. Summary of the safety and mission assurance category. Higher numbers are better.

Configuration	Abort & Reduncancy	# Mars Config Changes	# System Risks	**Total Rank**
Rigid Radial Spars	0.56	0.50	0.50	**0.52**
Trailing Torus	0.10	0.17	0.17	**0.14**
Tension Cone	0.10	0.17	0.17	**0.14**
Stacked Torus	0.25	0.17	0.17	**0.20**

The RRS configuration offers the significant advantage of providing an additional abort option over the inflatable configurations since it can be deployed prior to Earth departure and hence offers the option to not depart if the entry system does not deploy properly. The ST configuration offers a slight advantage over the other inflatable configurations since it has multiple independent air volumes, though failure of any of these volumes would likely reduce the drag area significantly and may still result in loss of mission or crew.

The number of Mars configuration transitions was minimum with the RRS configuration since it can be deployed prior to Earth departure, and does not require re-inflation between the aerocapture and entry events. All of the inflatable configurations require two inflations in the vicinity of Mars, compared to zero changes for the RRS configuration.

The RRS configuration offers a slight advantage to the inflatable configurations in the number and type of system risks and mission hazards as the lack of an inflatable volume provides additional resistance to micrometeoroids and orbital debris since it is not required to be air tight to function. Improved crew inspection of the deployed heatshield is also possible with the RRS configuration since the entry system can be deployed in advance, though this does increase the surface area for impact. In either case, a large impact will disable any of the entry vehicle configurations evaluated here.

Affordability & Life Cycle Cost

The affordability and life cycle cost category contains topics related to technology development costs and build costs. The main subtopics are cost to develop the required technologies to TRL 6, from TRL 6 to 8, and EDL related LCC. The EDL related LCC subtopic is further broken down into the entry system mass fraction, the stowed size of the entry system, and the complexity of the EDL system. A summary of the evaluations in this category is provided in Table 3 and rationales for the rankings are provided below.

Table 3. Summary of the affordability and life cycle cost category. Higher numbers are better.

Configuration	Cost to TRL6	Cost from TRL6 to 8	EDL-Related LCC			**Total Rank**
			Entry System Mass Fraction	Stowed Size of Entry System	Complexity of EDL System	
Rigid Radial Spars	0.25	0.38	0.35	0.07	0.25	**0.28**
Trailing Torus	0.10	0.13	0.19	0.39	0.25	**0.17**
Tension Cone	0.10	0.13	0.35	0.39	0.25	**0.18**
Stacked Torus	0.56	0.38	0.11	0.15	0.25	**0.37**

The cost to develop the ST configuration to TRL 6 is the lowest since it has successfully completed a sub-orbital velocity test flight. The RRS configuration follows this since a scale model was constructed at the Massachusetts Institute of Technology, but the launch vehicle failed, leaving the design unproven[ix]. The TT and TC configurations would be the most costly since they are still paper studies. The TT and TC configurations for a 100 mt entry mass also require an advance in manufacturing capability since their torus minor diameters are both larger than any facility in the world can currently braid.

The cost to develop each configuration from TRL 6 to 8 is higher for the TC and TT configurations since they require construction of larger braiding machines to construct their inflatable toroids. In other testing aspects, the configurations are equivalent since they are all deployable entry systems and will require nearly identical flight, ground, and wind tunnel tests to approximate Mars entry conditions.

The entry system mass fraction is an analog for the gross mass of the entry system that is typically used for system cost estimation. Entry system mass fraction is used since it was evaluated directly in the first portion of this study and can be directly scaled to the comparative scale used in AHP. Data was transformed to a 1 to 3 scale since the difference between all four configurations examined is relatively small. Since the ST configuration was not evaluated directly, its entry system mass fraction was calculated as 0.52 from data provided in the EDL-SA year 1 report. Since the assumptions of the EDL-SA study and the entry mass differ slightly relative to the HMMES study, the sensitivity to the ranking of the ST configuration was performed. This analysis determined that the overall ranking was unchanged when the ST configuration was changed from best to worst entry system mass fraction.

The stowed size of the entry system was best for the TT and TC configurations since they are inflatable and have less insulation than either the ST or RRS configurations. The ST configuration has a better packing size than the RRS configuration since the hollow radial spars cannot be crushed for packing and the radial spars were also not envisioned to have multiple hinges to keep complexity as low as possible.

The complexity of the EDL system is considered equivalent for all configurations. Both the mechanical and inflation systems require redundancy and are straightforward designs, similar to existing hardware.

Performance & Effectiveness

The performance and effectiveness category contains topics related EDL performance; entry system mass fraction and precision landing ability. The precision landing ability is further segmented into the ability to generate lift and the system's resistance to wind drift. The ability to precision land will be required for human-scale Mars missions in the current architecture where some assets are pre-positioned and the crew needs to land close to these assets. A summary of the evaluations in this category is provided in Table 4 and rationales for the rankings are provided below.

Table 4. Summary of the performance and effectiveness category. Higher numbers are better.

Configuration	Entry System Mass Fraction	Precision Landing		**Total Rank**
		Lift Generation	Wind Drift	
Rigid Radial Spars	0.35	0.56	0.38	**0.41**
Trailing Torus	0.19	0.10	0.13	**0.15**
Tension Cone	0.35	0.10	0.13	**0.23**
Stacked Torus	0.11	0.25	0.38	**0.21**

The entry system mass fraction analysis is described in the affordability and life cycle cost section (directly above). The resistance to wind drift was evaluated based on the class of the ballistic coefficient, which split into two groups; the ST and RRS configuration have a higher ballistic coefficient than the TT and TC configurations. A higher ballistic coefficient reduces the effect of the wind on the vehicle, so the ST and RRS configurations have a slight advantage in this category.

Lift generation is accomplished with either mass offset from the vehicle centerline, asymmetry of the geometry, or a combination of mass offset and geometry. The ability of the TT configuration to do either is somewhat limited, and is the most difficult configuration to generate moderate to high lift with. The TC configuration can accommodate some mass offset, but is not very stiff, and so is limited in the amount of lift that can be generated without unacceptable deformation of the vehicle. The ST configuration provides additional stiffness to support either mass offset or additional inflatable components to skew the geometry. The most suitable configuration for both mass offset and geometric asymmetry is the RRS configuration due to the rigid components increasing the stiffness and allowing direct control of the geometry. The direct control can be used to form the non-axisymmetric and relatively flat optimal entry shapes defined by Theisinger, Braun, and Clark[xix]. The RRS configuration provides a significant advantage for flat shapes since it does not rely on stiffness in the hoop-direction to maintain its shape. Control of the lift vector is also an issue, and the ST and RRS configurations have an advantage here due to their stiffer structures allowing the use of control flaps or thrusters mounted near the perimeter of the deployable.

Programmatic Risk

The programmatic risk category is composed of metrics that evaluate the difficulty to bring the technology to flight readiness, and the flight risks. The sub-topics are: level of EDL system maturity, TRLs of the required technologies, the research and development degree of difficulty, and the number of configuration changes required. A summary of the evaluations in this category is provided in Table 5 and rationales for the rankings are provided below.

Table 5. Summary of the programmatic risk category. Higher numbers are better.

Configuration	Level of EDL SystemMaturity	TRLs of Req'd Technologies	R&D^3 Score of Req'd Technologies	# of Config. Changes Req'd	**Total Rank**
Rigid Radial Spars	0.25	0.25	0.38	0.50	**0.34**
Trailing Torus	0.10	0.10	0.13	0.17	**0.12**
Tension Cone	0.10	0.10	0.13	0.17	**0.12**
Stacked Torus	0.56	0.56	0.38	0.17	**0.42**

The level of EDL system maturity is the highest for the ST configuration since it has a sub-orbital flight test under its belt, with the RRS configuration following close behind with its complete test article. The TT and TC configurations are only paper studies, and are far behind the ST and RRS configurations.

The TRL of required technologies for the ST configuration is the highest because it has been flight tested, albeit at a lower heat rate and load than that of a high mass Mars entry. The RRS configuration is the next highest since a test article has been constructed and ground tested. Technologies for the TT and TC configurations are the lowest as each requires some additional development, and neither has a flight test model designed or constructed. All of the configurations require additional development in the form of flexible TPS development for low to moderate heat rates.

The research and development degree of difficulty is similar for all configurations since this metric is dominated by flexible TPS development. There is additional cost associated with the TT and TC

configurations since they both require construction of larger braiding equipment at the 100 mt entry mass size, adding expense to enable testing of flight scale articles.

The number of configuration transitions required is the same metric described in the safety and mission assurance section, and is included here since geometry changes and actuation represent a significant risk. This metric favors the RRS configuration since it can be deployed prior to Earth departure and does not require re-inflation between aerocapture and entry maneuvers.

Applicability to Other Missions

The applicability to other missions category was intended to identify landing systems that are more broadly useful to NASA, but was ranked as relatively unimportant by program managers. In the current application of this metric to deployable entry systems (instead of EDL architectures) it is hard to differentiate the applicability to other missions since not all configurations have been analyzed at the same locations (other than Mars), yet enough of these configurations have been analyzed at different locations to see that they are not limited to high mass Mars applications. Since all of the configurations studied provide the same utility, it is difficult to argue that any one is more applicable to other missions, and so all are ranked equal.

Overall Rankings & Discussion

The overall result of applying AHP to the deployable entry system configurations using the top-level categories and weighting factors from the EDL-SA study are presented in Table 6. The highest ranked configuration is the rigid radial spars configuration, followed by the stacked torus configuration. The difference in ranking between the RRS and ST configurations was never more than a 3 (slight advantage), but the RRS configuration proved better in the safety and mission assurance and performance and effectiveness categories. In fact, the ST configuration is ranked higher than the RRS configuration in two of the five categories (and tied in one), but not by enough margin to overturn the highest ranking in the safety and mission assurance category, the most important category in program managers minds. The relatively large difference between the rankings of the RRS and ST configurations raises the question of whether the use of the RRS configuration in the EDL-SA study would change the outcome of the rigid versus deployable recommendation in the hypersonic flight regime.

Table 6. The RRS configuration tops the overall rankings of deployable entry systems.

Configuration	Overall Ranking	AHP Score
Rigid Radial Spars	1	0.40
Stacked Torus	2	0.27
Tension Cone	3	0.18
Trailing Torus	4	0.15

The TT and TC configurations are ranked the lowest overall. These two configurations suffer from a lack of redundancy and higher development costs since both are currently paper designs. They were also hurt by their configuration's lower ranking in the precision landing category since neither produce lift as easily

as the ST and RRS configurations, and both are more affected by the wind than the ST and RRS configurations.

Conclusions

A summary of the results of the HMMES study were presented, and the best configurations from that study were compared to the inflatable stacked torus configuration from the ELD-SA study, using the top-level categories and weightings from the EDL-SA study. These categories and weightings were chosen so that a comparison could be made to the study EDL-SA study results and because the categories and weightings were selected by NASA program managers, who represent the actual decision makers. The results of his comparison indicate that the rigid radial spar configuration has substantial advantages over the other configurations examined. The difference between the rankings of the RRS and ST configurations indicates that a change from the ST to RRS configurations in the EDL-SA study may change the relative ranking of the rigid and deployable hypersonic decelerators in the EDL-SA study, such that the deployable may be equal to or better than the rigid vehicle.

In examining the results of the ranking process, the RRS configuration has a significant advantage over other deployable configurations in the safety and mission assurance category, which program managers consider to be the most important category. The RRS configuration's advantage comes from its ability to deploy prior to Earth departure (since it is mechanical, and does not require re-fill gas), allowing an abort to LEO if the system fails to deploy, and simultaneously reduced the number of configuration changes at Mars to zero. The lack of inflation gas in the RRS configuration also provides better resistance to micrometeoroids, and the rigid radial spars enable easy lift generation through direct surface shaping, and control of the lift through thrusters or aerodynamic control surfaces near the perimeter of the deployable.

References

[i] Braun, R.D., and Manning, R.M., "Mars Exploration Entry, Descent, and Landing Challenges," *Journal of Spacecraft and Rockets*, Vol. 44, No. 2, pp. 310-323, 2007.

[ii] Miller, K.L., et al, "Trailing Ballute Aerocapture – Concept and Feasibility Assessment," AIAA Paper 2003-4655, 39th AIAA/ASME/SAE/ASEE Joint Propulsion Conference and Exhibit, Huntsville, AL, July 2003.

[iii] Zang, T.A., et al, "Overview of the NASA Entry, Descent and Landing Systems Analysis Study," AIAA Paper 2010-8649, AIAA Space 2010 Conference and Exposition, Anaheim, CA, Aug. 30-Sep. 2, 2010.

[iv] Rohrschneider, R.R., "High Mass Mars Entry System Final Report," Unpublished final report of contract NNL08AA34C, 2010.

[v] Otero, R.E., and Braun, R.D., "The Planetary Entry Systems Synthesis Tool: A Conceptual Design and Analysis Tool for EDL Systems," Paper #1331, IEEE Aerospace Conference, Big Sky, MT, 6-13 Mar., 2010.

[vi] Edquist, K.T., Prabhu, R.K., Hoffman, D.A., and Rea, J.R., "Configuration, Aerodynamics, and Stability Analysis for a Neptune Aerocapture Orbiter," AIAA Paper 2004-4953, AIAA Atmospheric Flight Mechanics Conference and Exhibit, Providence, RI, Aug. 2004.

[vii] Trabandt, U., Koeler, H., and Schmid, M., "Deployable CMC Hot Structure Decelerator for Aerobrake," AIAA Paper 2003-2169, 17th AIAA Aerodynamic Decelerator Systems Technology Conference and Seminar, Monterey, CA, May 19-22, 2003.

[viii] Product brochure from Forschungszentrum Jülich, "Carbon Fiber Reinforced Silicon Carbide (C/SiC), July 2004.

[ix] Akin, D.L., "The ParaShield Entry Vehicle Concept: Basic Theory and Flight Test Development," 4th Annual USU/AIAA Conference on Small Satellites, Utah State Univ., Logan, UT, Aug. 1990.
[x] Magazu, H.K., Lewis, M.J., and Akin, D.L., "Aerothermodynamics of a Parashield Re-Entry Vehicle," *Journal of Spacecraft and Rockets*, Vol. 35, No. 4, pp. 434-441, 1998.
[xi] Reza, S., Hund, R., Kustas, F., Willcockson, W., and Songer, J., "Aerocapture Inflatable Decelerator (AID) for Planetary Entry," AIAA Paper 2007-2516, 19th AIAA Aerodynamic Decelerator Systems Technology Conference and Seminar, Williamsburg, VA, May 2007.
[xii] Brown, G.J., Epp, C., Graves, C., Lingard, S., Darley, M., and Jordan, K., "Hypercone Inflatable Supersonic Decelerator," AIAA Paper 2003-2167, 17th AIAA Aerodynamic Decelerator Systems Technology Conference and Seminar, Monterey, CA, May 2003.
[xiii] "ESR&T Ultralightweight Ballute Final Report," NASA contract number NNL05AA30C, December 2, 2005.
[xiv] Miller, K.L., et al, "Ultralightweight Ballute Technology for Aerocapture and Aeroassist Missions," NASA-CR-1999-215248, Feb. 2008.
[xv] Spencer, D.A., et al. "Mars Pathfinder Entry, Descent, and Landing Reconstruction," *Journal of Spacecraft and Rockets,* Vol. 36 No. 3, pp. 357-366, 1999.
[xvi] Vanderplaats, G.N., *Numerical Optimization Techniques for Engineering Design*, Vanderplaats Research & Development, Inc., Colorado Springs, CO, 1999.
[xvii] Christian, J.A., Wells, G., Lafleur, J., Manyapu, K., Verges, A., Lewis, C., and Braun, R.D., "Sizing of an Entry, Descent, and Landing System for Human Mars Exploration," AIAA Paper 2006-7427, AIAA Space 2006 Conference, San Jose, CA, Sep. 2006.
[xviii] Dwyer Cianciolo, A.M., et al., "Entry, Descent and Landing Systems Analysis Study: Phase 1 Report," NASA/TM-2010-216720, July, 2010.
[xix] Theisinger, J.E., Braun, R.D., and Clark, I.G., "Aerothermodynamic Shape Optimization of Hypersonic Entry Aeroshells," AIAA Paper 2010-9200, 13th AIAA/ISSMO Multidisciplinary Analysis Optimization Conference, Fort Worth, TX, Sep. 13-15, 2010.